

The impact of nonlinear losses in the silicon micro-ring cavities on CW pumping correlated photon pair generation

Yuan Guo, Wei Zhang,* Ning Lv, Qiang Zhou, Yidong Huang, and Jiangde Peng

Tsinghua National Laboratory for Information Science and Technology, State Key Laboratory on Integrated Optoelectronics, Department of Electronic Engineering, Tsinghua University, Beijing 100084, China
*zwei@Tsinghua.edu.cn

Abstract: In this paper, 1.5 μm correlated photon pairs are generated under continuous wave (CW) pumping in a silicon micro-ring cavity with a Q factor of 8.1×10^4 . The ratio of coincidences to accidental coincidences (CAR) is up to 200 under a coincidence time bin width of 5ns. The experiment result of single side photon count shows that the generation rate does not increase as the square of the pump level due to the nonlinear losses in the cavity which reduce the Q factor and impact the field enhancement effect in the cavity under high pump level. Theoretical analysis shows that the photon pair generation rate in the cavity is proportional to the seventh power of the Q factor, which agrees well with the experiment result. It provides a way to analyze the performance of CW pumping correlated photon pair generation in silicon micro-ring cavities under high pump levels.

©2014 Optical Society of America

OCIS codes: (270.0270) Quantum optics; (190.4390) Nonlinear optics, integrated optics; (190.4380) Nonlinear optics, four-wave mixing.

References and links

1. J. E. Sharping, K. F. Lee, M. A. Foster, A. C. Turner, B. S. Schmidt, M. Lipson, A. L. Gaeta, and P. Kumar, "Generation of correlated photons in nanoscale silicon waveguides," *Opt. Express* **14**(25), 12388–12393 (2006).
2. Q. Lin, O. J. Painter, and G. P. Agrawal, "Nonlinear optical phenomena in silicon waveguides: modeling and applications," *Opt. Express* **15**(25), 16604–16644 (2007).
3. K. Harada, H. Takesue, H. Fukuda, T. Tsuchizawa, T. Watanabe, K. Yamada, Y. Tokura, and S. Itabashi, "Generation of high-purity entangled photon pairs using silicon wire waveguide," *Opt. Express* **16**(25), 20368–20373 (2008).
4. K. Harada, H. Takesue, H. Fukuda, T. Tsuchizawa, T. Watanabe, K. Yamada, Y. Tokura, and S. Itabashi, "Frequency and Polarization Characteristics of Correlated Photon-Pair Generation Using a Silicon Wire Waveguide," *IEEE J. Sel. Top. Quantum Electron.* **16**(1), 325–331 (2010).
5. A. J. Shields, "Semiconductor quantum light sources," *Nat. Photonics* **1**(4), 215–223 (2007).
6. Q. Lin and G. P. Agrawal, "Silicon waveguides for creating quantum-correlated photon pairs," *Opt. Lett.* **31**(21), 3140–3142 (2006).
7. S. M. Spillane, T. J. Kippenberg, and K. J. Vahala, "Ultralow-threshold Raman laser using a spherical dielectric microcavity," *Nature* **415**(6872), 621–623 (2002).
8. M. J. Thorpe, K. D. Moll, R. J. Jones, B. Safdi, and J. Ye, "Broadband cavity ringdown spectroscopy for sensitive and rapid molecular detection," *Science* **311**(5767), 1595–1599 (2006).
9. D. G. Rabus, Z. Bian, and A. Shakouri, "A GaInAsP-InP double-ring resonator coupled laser," *IEEE Photon. Technol. Lett.* **17**(9), 1770–1772 (2005).
10. E. Engin, D. Bonneau, C. M. Natarajan, A. S. Clark, M. G. Tanner, R. H. Hadfield, S. N. Dorenbos, V. Zwiller, K. Ohira, N. Suzuki, H. Yoshida, N. Iizuka, M. Ezaki, J. L. O'Brien, and M. G. Thompson, "Photon pair generation in a silicon micro-ring resonator with reverse bias enhancement," *Opt. Express* **21**(23), 27826–27834 (2013).
11. W. C. Jiang, X. Lu, J. Zhang, O. Painter, and Q. Lin, "A silicon-chip source of bright photon-pair comb." (2012). arXiv preprint arXiv:1210.4455
12. L. G. Helt, Z. Yang, M. Liscidini, and J. E. Sipe, "Spontaneous four-wave mixing in microring resonators," *Opt. Lett.* **35**(18), 3006–3008 (2010).

13. A. C. Turner, M. A. Foster, A. L. Gaeta, and M. Lipson, "Ultra-low power parametric frequency conversion in a silicon microring resonator," *Opt. Express* **16**(7), 4881–4887 (2008).
14. S. F. Preble, Q. Xu, and M. Lipson, "Changing the colour of light in a silicon resonator," *Nat. Photonics* **1**, 1293–1296 (2007).
15. S. Azzini, D. Grassani, M. J. Strain, M. Sorel, L. G. Helt, J. E. Sipe, M. Liscidini, M. Galli, and D. Bajoni, "Ultra-low power generation of twin photons in a compact silicon ring resonator," *Opt. Express* **20**(21), 23100–23107 (2012).
16. S. Clemmen, K. P. Huy, W. Bogaerts, R. G. Baets, P. Emplit, and S. Massar, "Continuous wave photon pair generation in silicon-on-insulator waveguides and ring resonators," *Opt. Express* **17**(19), 16558–16570 (2009).
17. N. M. Wright, D. J. Thomson, K. L. Litvinenko, W. R. Headley, A. J. Smith, A. P. Knights, J. H. B. Deane, F. Y. Gardes, G. Z. Mashanovich, R. Gwilliam, and G. T. Reed, "Free carrier lifetime modification for silicon waveguide based devices," *Opt. Express* **16**(24), 19779–19784 (2008).
18. S. Azzini, D. Grassani, M. Galli, L. C. Andreani, M. Sorel, M. J. Strain, L. G. Helt, J. E. Sipe, M. Liscidini, and D. Bajoni, "From classical four-wave mixing to parametric fluorescence in silicon microring resonators," *Opt. Lett.* **37**(18), 3807–3809 (2012).
19. L. G. Helt, M. Liscidini, and J. E. Sipe, "How does it scale? comparing quantum and classical nonlinear optical processes in integrated devices," *J. Opt. Soc. Am. B* **29**(8), 2199–2212 (2012).
20. B. E. Little, S. T. Chu, H. A. Haus, J. Foresi, and J.-P. Laine, "Microring Resonator Channel Dropping Filters," *J. Lightwave Technol.* **15**(6), 998–1005 (1997).
21. A. R. Motamedi, A. H. Nejadmalayeri, A. Khilo, F. X. Kärtner, and E. P. Ippen, "Ultrafast nonlinear optical studies of silicon nanowaveguides," *Opt. Express* **20**(4), 4085–4101 (2012).
22. D. G. Rabus, *Integrated ring resonators* (Springer, Berlin, 2007).
23. M. Soltani, *Novel integrated silicon nanophotonic structures using ultra-high Q resonator*, Ph.D. dissertation, Georgia Institute of Technology, 2009.
24. M. Ferrera, L. Razzari, D. Duchesne, R. Morandotti, Z. Yang, M. Liscidini, J. E. Sipe, S. Chu, B. E. Little, and D. J. Moss, "Low-power continuous-wave nonlinear optics in doped silica glass integrated waveguide structures," *Nat. Photonics* **2**(12), 737–740 (2008).
25. P. P. Absil, J. V. Hryniewicz, B. E. Little, P. S. Cho, R. A. Wilson, L. G. Joneckis, and P. T. Ho, "Wavelength conversion in GaAs micro-ring resonators," *Opt. Lett.* **25**(8), 554–556 (2000).

1. Introduction

Correlated photon pairs have important applications in quantum information and quantum communication. In recent years, spontaneous four wave mixing (SFWM) in silicon wire waveguides attracts much attention for its potential to realize correlated photon pair generation in 1.5 μm band [1]. The nonlinear coefficient of silicon wire waveguides is about five magnitudes higher than silica fibers thanks to their ultra-small modal field areas and the high Kerr nonlinearity n_2 of silicon material [2]. On the other hand, since the spectrum of spontaneous Raman scattering in a silicon wire waveguide is quite narrow, the noise photons induced by spontaneous Raman scattering are easy to be filtered out, which is effective for realizing low noise correlated photon pair generation at room temperature [3]. Furthermore, silicon wire waveguides can be fabricated by standard CMOS process, indicating the potential on developing silicon integrated quantum light sources [4]. Hence, silicon waveguide has been widely investigated as an important scheme for 1.5 μm correlated photon pair generation [5,6].

Micro-ring cavities [7–9] based on silicon wire waveguide are important silicon device structures. If the input light is at the resonance wavelength of a cavity mode, the light field in the cavity would be enhanced significantly, leading to a significant improvement of the efficiency of correlated photon pair generation [10,11]. A micro-ring cavity with a circumference of several tens of micrometers could generate correlated photon pairs effectively [12]. Comparatively, for simple silicon waveguides without micro-ring structures, samples of several millimeters or 1–2 centimeters in length are required. The light field enhancement in the cavities can reduce the requirement of input pump power [13–15] because it not only reduces the difficulty in the residual pump suppression but also significantly reduces the noise photons generated by the spontaneous Raman scattering in optical fibers, such as pigtailed of optical components and the lensed fibers in the experiment setup. As a result, correlated photon pair generation under CW pumping can be effectively realized in silicon micro-ring cavities [16]. However, the light field enhancement would also increase the nonlinear loss in the cavity such as the two-photon absorption (TPA) and free carrier

absorption (FCA) in the silicon materials. The nonlinear loss reduces the Q factor of the cavity, which would impact the correlated photon pair generation in the cavity. In this paper, 1.5 μm correlated photon pair generation is realized in a silicon micro-ring cavity under CW pumping at room temperature. The setup description and results of the experiment are shown in section 2. The impact of the nonlinear loss in the cavity is analyzed in Section 3. Section 4 is the conclusion.

2. Experiment of correlated photon pair generation in a silicon micro-ring cavity under CW pumping

The silicon micro-ring cavity is fabricated by standard CMOS processes (by Institute of Microelectronics, Singapore). Its sketch is shown in Fig. 1(a). The ring has a shape of racetrack, with a circumference of 132.5 μm . It is coupled to a bus waveguide, which is 3 mm in length. The cross section of the bus waveguides and ring is depicted in Fig. 1(b).

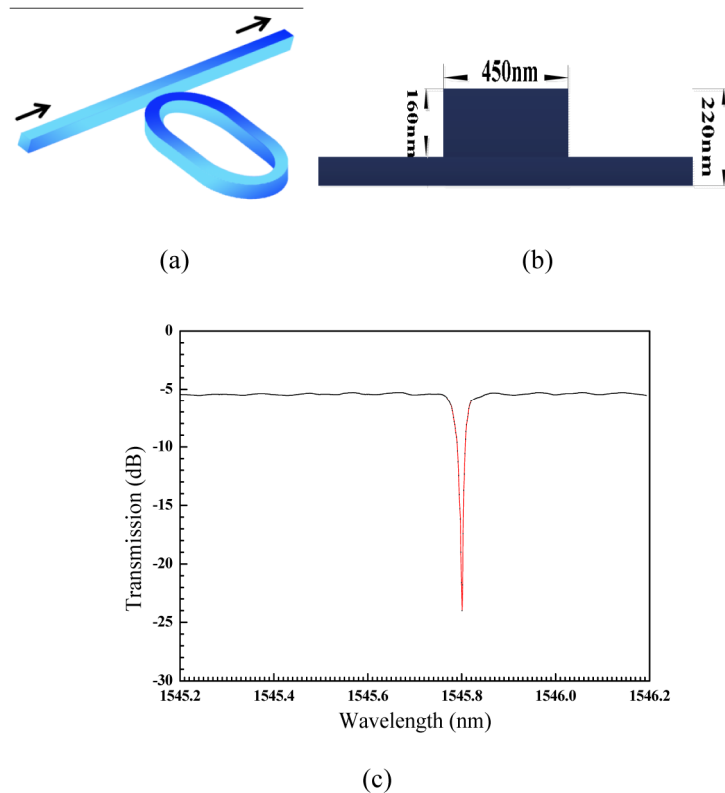


Fig. 1. The micro-ring cavity used in the experiment. (a) The sketch of the cavity, (b) The cross section of the bus waveguide and the waveguide in the cavity. (c) The transmission spectrum of the quasi-TE mode near the resonance wavelength of a specific cavity mode.

The transmission spectrum of the cavity is measured under low probe light power by an optical device measurement system with a tunable laser (TSL510, Santec Inc.) and a power meter (Agilent 8164B). Inverted taper structures are fabricated at both ends of the bus waveguide to reduce the coupling loss between the waveguide and the lensed fibers. Figure 1(c) shows the measured spectrum of the quasi-transverse electrical mode (TE) near the resonance wavelength. The black dots are experiment results and the red line is the result of Lorentz fitting. It can be seen that the insertion loss of the bus waveguide is 5.6 dB, shown by the off-resonance transmission value. A narrow dip appears at the resonance wavelength with an extinction ratio of 19 dB. The full width of half maximum (FWHM) of the resonance dip is

0.019nm, showing a Q factor of 8.1×10^4 , estimated by the ratio between the resonance wavelength and the FWHM.

The experiment setup for the correlated photon pair generation in the micro-ring cavity is shown in Fig. 2. The tunable laser (TSL510, Santec Inc.) is used as the CW pump source. Its wavelength is tuned to the resonance wavelength shown in Fig. 1(c). Two cascaded tunable filters are used to improve the side band rejection of the pump light up to 130dB. The pump light is injected into the bus waveguide as quasi-TE mode by a polarization controller (PC). It generates signal and idler photons in two cavity modes near the mode for the pump light. The generated photon pairs are separated by a filter system including a coarse wavelength division multiplexing (CWDM) device and several tunable filters. The center wavelengths of the filter systems for the signal and idler photons are tuned to 1537.05 nm and 1554.66 nm, respectively, corresponding to the resonance wavelength of two cavity modes for the signal and idler photons. The transmission losses of the filter system are 4.1dB and 4.3dB for the signal and idler photons, respectively. Then the signal and idler photons are detected by two free running single photon detectors (SPDs, Id220, IDQ, Inc.). Their detection efficiencies and dead times are set as 10% and 10 μ s, respectively.

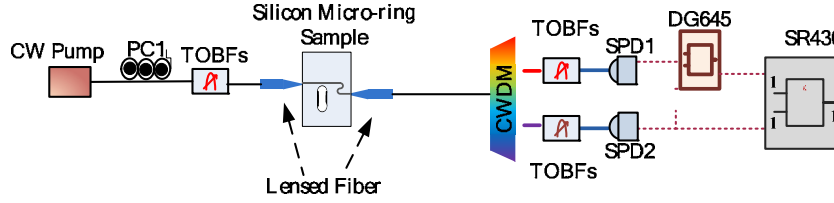


Fig. 2. The experiment setup for the correlated photon pair generation in the micro-ring cavity. PC, polarization controller; TOBF, tunable optical band-pass filter; SPD, single photon detector; CWDM, coarse wavelength division multiplexer.

Firstly, the signal side photon count rate is measured under different pump levels and plotted in Fig. 3 as the black squares. In the measurement, the pump light is always tuned to the resonance wavelength of the cavity mode under each pump level. It can be seen that the count rate rises with increasing pump level. However, it is saturated by the dead time of the single photon detector. Actually, the generation rate of signal photons at the output end of the bus waveguide should be calculated by

$$R_s = C'_s / \eta_s \quad (1)$$

Where η_s is the collection and detection efficiency at signal side, including the detection efficiency of the SPD and the transmission efficiency between the output end of the bus waveguide and the SPD. C'_s has the same unit as the measured signal side count rate (denoted by C_s) and is calculated by

$$C'_s = \frac{C_s - d_s}{1 - C_s \tau_s} \quad (2)$$

Where, d_s and τ_s are the dark count rate and the dead time of the signal side SPD, respectively. It can be seen that C'_s is a modified signal side count rate proportional to R_s , in which the impacts of dead time and dark count of the SPD are taken out. The blue dots in Fig. 3 are the calculated C'_s according to the measured signal side count rate. It can be seen that C'_s is close to C_s at low pump level, while far higher than C_s at high pump level.

Previous theoretical works have shown that the correlated photon pair generation rate in a micro-ring cavity is proportional to $P_p^2 Q^3$, where P_p is the input pump power and Q is the quality factor of the micro-cavity. Under low pump level, it can be expected that R is

proportional to P_p^2 (so is C'_s) since Q factor can be looked as a constant. The C'_s measured under an input pump powers lower than 0.1mW are fitted by the function of $AP_p^2Q^3$ and the curve is then extended to high pump power which is shown as the red line in Fig. 3. In the curve fitting Q is set as a constant 8.1×10^4 and A is the fitting parameter. The inset figure in Fig. 3 is the detailed fitting result at low pump level. It can be seen that although the curve fitting has high precision at low pump level, it overestimates the C'_s under a high pump level. The reason for this overestimation is that the Q factor of the cavity would reduce if the pump level is high enough to introduce obvious nonlinear loss in the cavity [17]. Its impact on the correlated photon pair generation will be analyzed comprehensively and shown in section 3.

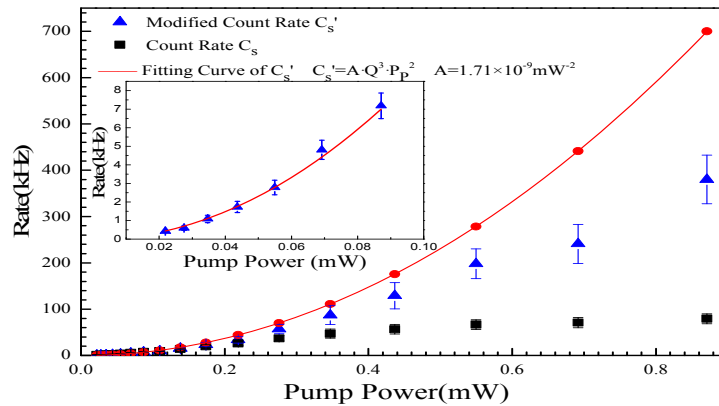
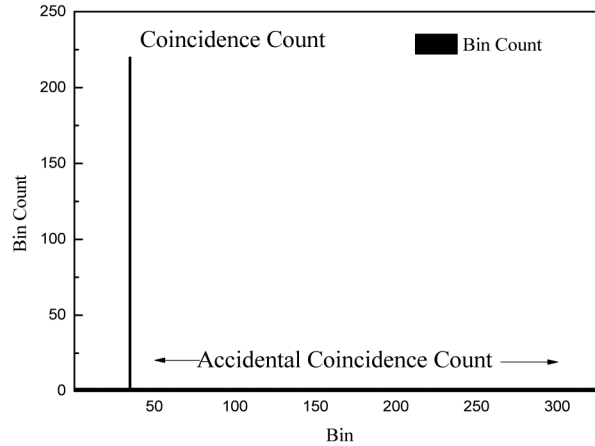
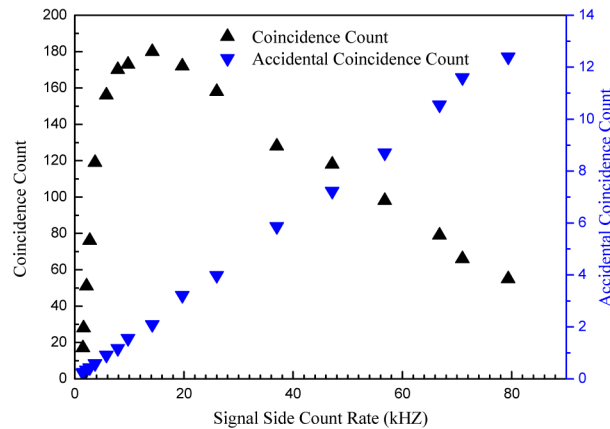


Fig. 3. Signal side photon count rates under different input pump power. The black squares: measured count rate C_s ; The blue dots: modified count rate C'_s . The red line: the fitting curve of the C'_s with an input pump power lower than 0.1mW utilizing $AP_p^2Q^3$. The inset figure: the detail fitting result at low pump level.

The quantum correlation between the signal and the idler photons is demonstrated by the measurement of coincidence count and accidental coincidence count, which are shown in Fig. 4. The output of the signal side SPD is connected to the multi-channel scalar (SR-430, Stanford Scientific Research, Inc) as the trigger signal. The output signal of the idler side SPD is connected to the multi-channel scalar with a time delay induced by a digital delay generator (DG-645, Stanford Scientific Research, Inc). The time delay, time bin width and the total trigger number are set as 180ns, 5ns, 30000, respectively. Figure 4(a) shows a typical result of a coincidence count measurement. The correlation between the generated photon pairs leads to an obvious high counts in a specific time bin, which is recorded as the coincidence count. The average count of tens of time bins nearby is calculated as the accidental coincidence count. The measurement results of the coincidence and accidental coincidence counts under different signal side count rate are shown in Fig. 4(b). Theoretically, the coincidence count should be a constant under different signal side count rate C_s , which is determined by the collection and detection efficiencies of the generated idler side photons. However, the coincidence count reduces rapidly with decreasing pump level when pump power is low due to the impact of dark counts of the SPD1. It also reduces with increasing pump level when pump power is high, which may be due to the impact of the dead time of the SPD2. On the other hand, the accidental coincidence count is proportional to the signal side count rate.



(a)



(b)

Fig. 4. Measured results of the coincidence count and accidental coincidence count. (a) a typical result of a coincidence count measurement; (b) Coincidence and accidental coincidence counts under different signal side count rate; Black triangles: the coincidence counts; Blue triangles: the accidental coincidence counts.

The CAR under different signal side count rate is shown in Fig. 5. It can be seen that the CAR increases with decreasing signal side count rate-under high pump level. However, it reduces rapidly at low pump level due to the dark counts of SPD1. Usually, the performance of the experiment setup for correlated photon pair generation can be evaluated by the maximum CAR it achieves. It can be seen that the maximum CAR is as high as 200 in the experiment. Since relatively large time bin (5ns) is used in the experiment, such a high CAR is owe to the excellent isolation of the residual pump light and spontaneous Raman noise photons, low insertion loss of the micro-ring cavity sample and high collection efficiencies of generated signal and idler photons.

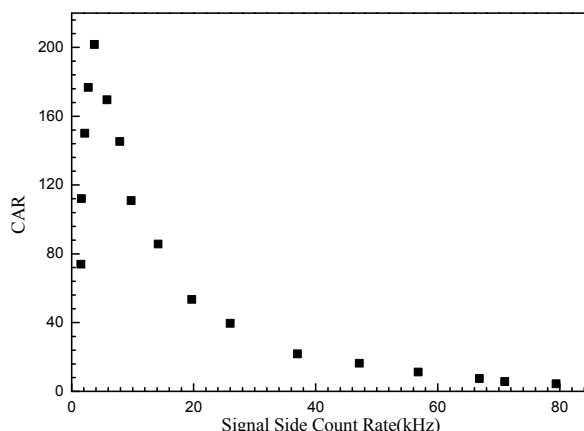


Fig. 5. The measured CAR under different signal side count rate.

3. The impact of nonlinear losses in silicon micro-ring cavities on the CW pumping correlated photon pair generation

Figure 3 has indicated that the generation rate does not increase as the square of the pump level due to the impact of nonlinear losses in the silicon micro-ring cavity. In previous theoretical analysis, Q factor of the cavity is always considered as a constant to simplify the relation between the photon pair generation rate and the pump level [18,19]. However, it is not suitable to analyze the photon pair generation rate under high pump level, since the intrinsic Q factor of the cavity changes due to the nonlinear loss in the cavity. In this section, the impact of the nonlinear loss on the relation between the photon pair generation rate and the pump level is investigated.

The light propagation in the silicon waveguide can be described by

$$\frac{dP}{dz} = -\alpha_{eff} P \quad (3)$$

$$\alpha_{eff} = \alpha + \frac{\beta P}{A_{eff}} + \frac{\tau \beta \sigma P^2}{2h\nu A_{eff}} \quad (4)$$

Where, P is the light power propagates in the silicon waveguide. The total waveguide loss coefficient, which is denoted by an effective loss coefficient α_{eff} , has three contributions: the first one is the linear loss, which is expressed by a linear loss coefficient α . The second one is the two-photon absorption (TPA) effect of silicon, which is expressed by the TPA coefficient β . The last one is the free carrier absorption (FCA) effect of silicon, which can be expressed through the FCA cross section σ and free carrier recombination life τ . A_{eff} , ν , h are the effective area of the silicon waveguide, the light frequency and the Planck constant, respectively.

For a micro-ring cavity coupled to a bus waveguide, the Q factor of a specific cavity mode can be expressed as [20]

$$1/Q = 1/Q_e + 1/Q_0 \quad (5)$$

Where Q_0 and Q_e are the intrinsic and external Q factor of the cavity mode, respectively. Q_0 can be calculated by Eq. (6), in which α_{eff} is the effective loss coefficient of the waveguide in

the cavity, v_g is the group velocity of the light propagating in the cavity and ω is the angular frequency of the light.

$$Q_0 = \frac{\omega}{\alpha_{eff} v_g} \quad (6)$$

Q_e can be calculated by Eq. (7), in which κ is the coupling coefficient between the cavity and the bus waveguide, L is the circumference of the cavity, while L/v_g is the round trip time of the light in the cavity

$$Q_e = \frac{\omega L}{|\kappa|^2 v_g} \quad (7)$$

In experiments, the Q factor of a specific cavity mode is usually estimated through the transmission spectrum near the resonance wavelength of the mode, which can be measured by a tunable laser with low power. If the Q factor is high ($Q \gg 1$), it can be estimated by the ratio between the resonance wavelength λ and line width $\Delta\lambda$ of the dip shown in the spectrum

$$Q = \frac{\lambda}{\Delta\lambda} \quad (8)$$

If both Q_0 and Q_e are far higher than 1, it can be deduced that the extinction ratio (denoted by Γ) can be expressed as (the derivation is shown in the appendix)

$$\Gamma \approx \left| \frac{Q_e - Q_0}{Q_e + Q_0} \right|^2 \quad (9)$$

Hence, after the estimation of Q factor by Eq. (8), the Q_0 and Q_e of the mode also can be calculated according to the transmission spectrum through Eqs. (5) and (9). For the micro-ring cavity sample used in our experiment, the Q , Q_0 and Q_e of the specific mode can be calculated according to the measured transmission spectrum shown in Fig. 1(c), which are 8.1×10^4 , 14.6×10^4 and 18.3×10^4 , respectively. However, this method can't be used to analyze the cavity under high light power due to strong light field enhancement effect in the cavity. On one hand, it will lead to obvious nonlinear losses in the cavity, which will change the intrinsic Q factor of the cavity. On the other hand, the index of the silicon waveguide in the cavity also changes under high light power, leading to a resonance wavelength shift of the cavity mode.

To investigate the impact of nonlinear loss in the cavity on the photon pair generation rate, we calculate the value of Q_0 under different pump level according to the parameters of micro-ring cavity sample and parameters of TPA and FCA in silicon material. Equation (6) shows the relation between the Q_0 and the effective loss coefficient α_{eff} , which includes the contribution of nonlinear losses. The definition of α_{eff} is shown in Eq. (4). In the following calculation, β , σ and τ are set as $6.7 \times 10^{-12} \text{m/W}$, $1.97 \times 10^{-21} \text{m}^2$ and 4ns respectively according to the parameters of bulk silicon material [21]. The A_{eff} is $0.1 \mu\text{m}^2$, calculated according to the parameters of the waveguide cross section. ν is frequency of the pump light.

In Eq. (4), α is the linear loss coefficient. Under low light power, nonlinear losses can be neglected and the α_{eff} is simplified to α . Hence, according to the measured Q_0 under low light power, α of the waveguide in the cavity can be calculated as 1.14dB/cm by Eq. (4). In the calculation, v_g is $c/4.12$ calculated by the expression of $v_g = c/n_g = c \times L \times \Delta\lambda_{FSR}/\lambda^2$ [22], where c is the light speed in vacuum, the cavity circumference L is $132.5 \mu\text{m}$, $\Delta\lambda_{FSR}$ is the free spectrum region (FSR) of the cavity, which is measured as 4.4nm.

If the light power in the cavity is high, the contributions of FCA and TPA can't be neglected. The light power circling in the cavity can be expressed by

$$P_c = P_{in} |F(\omega)|^2 \quad (10)$$

Where P_{in} is the light power in the bus waveguide before coupled to the ring. $F(\omega)$ is the field enhancement factor of the cavity [23] under the light frequency ω . If the input light is close to resonance wavelength, it can be expressed as

$$|F(\omega)|^2 = \frac{v_g}{L\omega} \cdot \frac{4/Q_e}{(\omega - \omega_0)^2 / \omega_0^2 + (1/Q_e + 1/Q_0)^2} \quad (11)$$

Considering that the pump light in the experiment is always on resonance, the field enhancement factor of the pump light, which is denoted by F_p , can be expressed as

$$|F_p|^2 = \frac{v_g}{L\omega_p} \cdot \frac{4/Q_e}{(1/Q_e + 1/Q_0)^2} \quad (12)$$

Where ω_p is the angular frequency of the pump light.

Equation (7) shows that Q_e is determined by the coupling coefficient κ , which does not change with the pump level. Substituting the expression of P_c (Eqs. (10) and (12)) into Eq. (3) and Eq. (4), it can be seen that the nonlinear loss coefficient α_{eff} in the cavity is a function of P_{in} and Q_0 . Substituting this expression of α_{eff} into Eq. (6), the relation between P_{in} and Q_0 can be derived and Q_0 under different input pump level can be calculated. Figure 6 shows the calculated Q_0 , Q and Q_e under different input pump power, which are plotted as the lines with squares, circles and triangles, respectively. In this figure, the power of the pump source is used as the horizontal axis, which is 2.8dB higher than P_{in} estimated by the coupling efficiency between the input lensed fiber and the bus waveguide. It can be seen that due to the nonlinear losses in the micro-ring cavity, Q_0 decreases with increasing pump level, while, Q_e is unchanged. As a result, the total Q also decreases with increasing pump level due to the nonlinear losses in the cavity. Q_0 is lower than Q_e under all the pump levels, showing that the cavity used in the experiment is under-coupling.

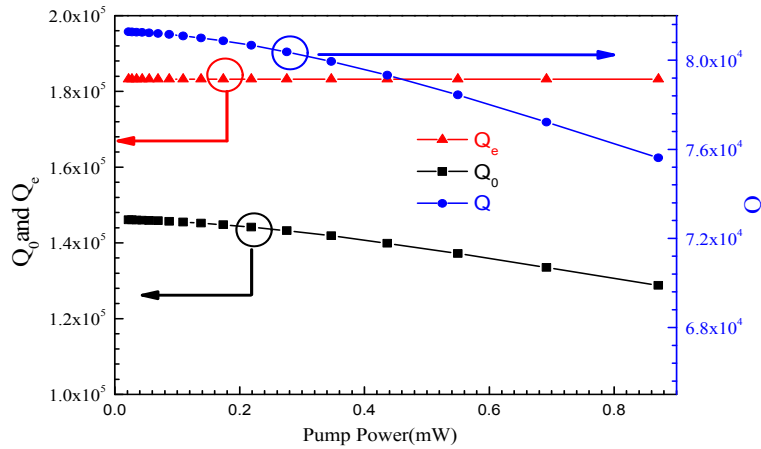


Fig. 6. Calculated Q , Q_0 and Q_e under different input pump power.

In the experiment of correlated photon pair generation in micro-ring cavities, the pump light is always tuned on resonance for a specific cavity mode, the signal and idler photons generated in two cavity modes symmetrical to the pump wavelength are detected. The field

enhancement effects of the pump light, signal photons and idler photons all affect the photon pair generation rate [24,25]. Since the modes for pump light, signal photons and idler photons are close in frequency, it can be assumed that they have the same Q_e and Q_o . Previous theoretical analysis [19] has shown that the P_l , which is the average power associated with half of the generated photons due to the SFWM, can be expressed by

$$P_l = \frac{h\omega_p}{T} (\gamma P_{in} L)^2 |F_p|^4 \quad (13)$$

Where F_p is calculated by Eq. (12). γ is the nonlinear coefficient of the silicon waveguide, T^{-1} is the bandwidth of the generated photons by SFWM. In the case of micro-ring cavities, T is calculated by

$$T = \frac{2\pi}{\int d\Delta\omega |F(\omega_0 - \Delta\omega)|^2 |F(\omega_0 + \Delta\omega)|^2} \quad (14)$$

under the assumption that $\omega_s \approx \omega_i \approx \omega_p = \omega_0$. Considering that the signal frequency ω_s and idler frequency ω_i satisfy that $\omega_s + \omega_i = 2\omega_p$, $\Delta\omega$ is defined as $\Delta\omega = \omega_s - \omega_{0,s} = \omega_{0,i} - \omega_i$, $\omega_{0,s}$ and $\omega_{0,i}$ are resonance frequency of the cavity modes for the signal and idler photons, respectively. Substituting Eq. (11) into Eq. (13) and Eq. (14), it can be calculated that,

$$T = \frac{Q_e^2 L^2 \omega_{p0}}{4\pi v_g^2 Q^3} \quad \text{hence,} \quad P_l = \frac{2\hbar(\gamma P_{in})^2 v_g^4 Q^7}{L^2 \omega_p^2 Q_e^4} \quad (15)$$

Hence, $R \propto P_l \propto P_p^2 Q^7$.

It is worthwhile to note that if the cavity satisfies the critical coupling condition, i.e. $Q_o = Q_e$, this relation would be simplified to $R \propto P_p^2 Q^3$. Another simplification usually used in some condition is to ignore the intrinsic loss of the cavity, i.e. $Q = Q_e$, it also leads to $R \propto P_p^2 Q^3$. In both cases, it is supposed that Q factor of the cavity is constant and the nonlinear losses in the cavity are not considered.

The analysis in section 2 has shown that the modified signal side count rate C' in the experiment is proportional to the photon pair generation rate R . Figure 3 has shown that $R \propto P_p^2 Q^3$ does not make a decent description of the relation between the photon pair generation rate and pump level when the pump power is high. The theoretical analysis in this section shows that under high pump level, the reduction of the Q factor due to the nonlinear losses in the cavity should be considered, leading to the relation of $R \propto P_p^2 Q^7$. To demonstrate it, the C' measured under an input pump power lower than 0.1mW are fitted by the function of $C' = BP_p^2 Q^7$. B is the fitting parameter. The value of Q utilizes the calculated results shown in Fig. 6, in which the nonlinear losses due to the FCA and TPA in the cavity are considered. The fitting result is shown in Fig. 7, while the fitting result of $C' = AP_p^2 Q^3$ in Fig. 3 is also plotted for comparison. It can be seen that compared with the results of $C' = AP_p^2 Q^3$, the fitting result of $C' = BP_p^2 Q^7$ not only has a high precision at low pump level, but also agrees well with the C' at high pump level. The comparison shows that under high pump level, the relation between the photon pair generation rate and pump level should be described by Eq. (15) or $R \propto P_p^2 Q^7$, in which the Q factor reduces with increasing pump level due to the nonlinear losses in the cavity.

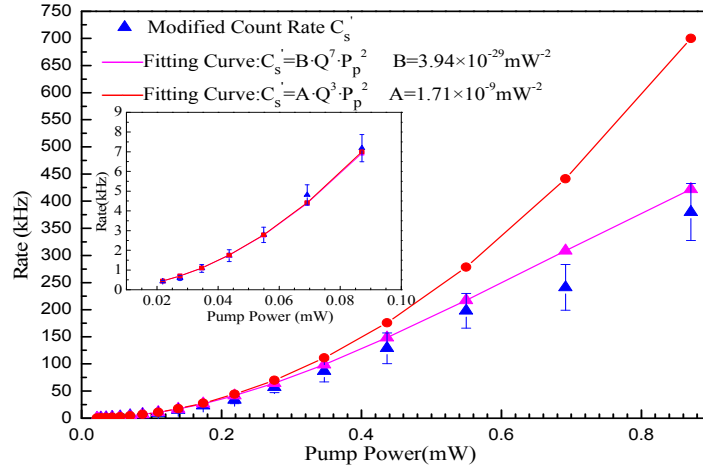


Fig. 7. Fitting results of the modified signal side photon count rates under different input pump power. The blue triangle: modified count rate C_s' . The red dots and magenta triangles: the fitting result of $C_s'' = AP_p^2Q^3$ and $C_s' = BP_p^2Q^7$, respectively.

4. Conclusion

In this paper, $1.5\mu\text{m}$ correlated photon pairs are generated under CW pumping in a silicon micro ring cavity with a Q factor of 8.1×10^4 . The measured CAR is up to 200 under a coincidence time bin width of 5ns. The Experiment results show that the photon pair generation rate does not increase as the square of the pump level due to the nonlinear losses in the silicon micro-ring cavity. Theoretical analysis shows that the relation between the photon pair generation rate and the pump level should be described by $R \propto P_p^2 Q^7$, meanwhile, the Q factor reduces with increasing pump level. This relation agrees well with the experiment results, providing a way to analyze the performance of the correlated photon pair generation in silicon micro-ring cavities at high pump level.

5. Appendix

The transmission of a bus waveguide with a micro-ring cavity can be expressed as

$$\Gamma = \left| \frac{t - \Lambda \exp(i\beta L)}{1 - \Lambda t \exp(i\beta L)} \right|^2 \quad (16)$$

Where, β is the light propagation constant in the micro-ring cavity. t is the field straight-through coupling coefficient and Λ is the round trip loss coefficient of resonator. In a high Q

cavity, they can be simplified as $t = \sqrt{1 - |\kappa|^2} \approx 1 - \frac{|\kappa|^2}{2}$ and $\Lambda = \exp\left(-\frac{\alpha_{\text{eff}} L}{2}\right) \approx 1 - \frac{\alpha_{\text{eff}} L}{2}$

according to $|\kappa|^2 \ll 1$ and $\alpha_{\text{eff}} L / 2 \ll 1$, where κ is the field cross-coupling coefficient.

If the input light is on resonance, according to Eqs. (6) and (7), equation (16) can be simplified as:

$$\Gamma = \left| \frac{t - \Lambda}{1 - \Lambda t} \right|^2 \approx \left| \frac{\exp\left(-\frac{\alpha_{eff} L}{2}\right) - \sqrt{1 - |\kappa|^2}}{1 - \exp\left(-\frac{\alpha_{eff} L}{2}\right) \cdot \sqrt{1 - |\kappa|^2}} \right|^2 \approx \left| \frac{\frac{\alpha_{eff} L}{2} - \frac{|\kappa|^2}{2}}{1 - \left(1 - \frac{\alpha_{eff} L}{2} - \frac{|\kappa|^2}{2} + \frac{\alpha_{eff} L}{2} \cdot \frac{|\kappa|^2}{2}\right)} \right|^2 \quad (17)$$

$$\approx \left| \frac{\alpha_{eff} L - |\kappa|^2}{\alpha_{eff} L + |\kappa|^2} \right|^2 = \left| \frac{Q_e - Q_0}{Q_e + Q_0} \right|^2$$

Acknowledgment

This work is supported in part by 973 Programs of China under Contract No. 2011CBA00303 and 2010CB327606, Tsinghua University Initiative Scientific Research Program, Basic Research Foundation of Tsinghua National Laboratory for Information Science and Technology (TNList), and China Postdoctoral Science Foundation.